
Article:
Sala, E.M. orcid.org/0000-0001-8116-8830, Bollani, M., Bietti, S. et al. (3 more authors) (2014) Ordered array of Ga droplets on GaAs(001) by local anodic oxidation. Journal of Vacuum Science & Technology B, Nanotechnology and Microelectronics: Materials, Processing, Measurement, and Phenomena, 32 (6). 061206. ISSN 2166-2746

https://doi.org/10.1116/1.4901017

JVSTB Journal of Vacuum Science & Technology B

Ordered array of Ga droplets on GaAs(001) by local anodic oxidation

Elisa M. Sala, Monica Bollani, Sergio Bietti, Alexey Fedorov, Luca Esposito, and Stefano Sanguinetti

Citation: Journal of Vacuum Science & Technology B **32**, 061206 (2014); doi: 10.1116/1.4901017
View online: http://dx.doi.org/10.1116/1.4901017
View Table of Contents: http://scitation.aip.org/content/avs/journal/jvstb/32/6?ver=pdfcov
Published by the AVS: Science & Technology of Materials, Interfaces, and Processing

Ordered array of Ga droplets on GaAs(001) by local anodic oxidation

Elisa M. Sala
L-NESS and Dipartimento di Scienza dei Materiali, Università di Milano-Bicocca, via Cozzi 53, I-20125 Milano, Italy

Monica Bollani
CNR-IFN, L-NESS, via Anzani 42, I-22100 Como, Italy

Sergio Bietti[a)]
L-NESS and Dipartimento di Scienza dei Materiali, Università di Milano-Bicocca, via Cozzi 53, I-20125 Milano, Italy

Alexey Fedorov
CNR-IFN, L-NESS, via Anzani 42, I-22100 Como, Italy

Luca Esposito and Stefano Sanguinetti
L-NESS and Dipartimento di Scienza dei Materiali, Università di Milano-Bicocca, via Cozzi 53, I-20125 Milano, Italy

(Received 3 July 2014; accepted 22 October 2014; published 4 November 2014)

The authors present a procedure to obtain uniform, ordered arrays of Ga droplets on GaAs(001) substrates. The growth process relies on an interplay between the substrate patterning, in form of a two dimensional array of nanoholes periodically modulated obtained via local anodic oxidation, and self-assembly of Ga droplets in a molecular beam epitaxy environment. The formation of site controlled Ga droplets, characterized by atomic force microscopy, is the outcome of the combined effects of capillary condensation and nucleation kinetics. © *2014 American Vacuum Society*. [http://dx.doi.org/10.1116/1.4901017]

I. INTRODUCTION

Self-assembled quantum dots (QDs) are semiconductor nanostructures relevant for applications ranging from lasers[1,2] to single photon sources for quantum communication.[3] GaAs/AlGaAs QDs grown by droplet epitaxy (DE)[4,5] technique are attractive for these applications, allowing to fabricate, by self-assembly, strain-free nanostructures with controllable density and shape,[6–8] at a low thermal budget[9] also suitable for the integration on CMOS technology.[10]

DE technique is based on a two-step procedure. In the first one, self-assembled nanoscale droplets are formed on the substrate by supplying a molecular beam of group III element. In the second step, the substrate is exposed to group V element, leading to spontaneous crystallization of the droplets into III–V nanocrystals. In the case of GaAs nanostructures, Ga droplets can be deposited on Ga(Al)As flat surface[11–15] or by infilling nanoholes created by *in situ* droplet etching.[16–19] Both methods rely on spontaneous nucleation of Ga droplets, which results in random dot positions. This could be a limitation for photonic applications, which require spatial and spectral matching of the QD position with the confined optical modes of optical waveguides or resonators.[20]

Several methods were already reported in scientific literature for the site controlled nucleation of III–V QDs on a patterned surface.[21] In the case of GaAs substrates, the localization of InAs nanostructures grown by Stranski–Krastanow technique could be of particular interest. Standard e-beam lithography and reactive ion etching was used by Heidemeyer *et al.*,[22] e-beam lithography with wet etching by Atkinson *et al.*,[23] and interferometric lithography and dry etching to fabricate SiO_2 masks by Tran *et al.*[24] Anyway, lithographic techniques require the use of resist and etching procedures, which introduce impurities and defects during the patterning process.[25] For this reason, local anodic oxidation (LAO)[26–28] was proposed to reduce the contaminants into the nanoholes and at the interface. In particular, the fabrication of InAs QDs on patterned substrates obtained with LAO technique was reported, e.g., by Kim *et al.*[27] and Alonso-Gonzalez *et al.*[25]

Here we present a method to localize Ga droplets on GaAs(001) surface at a specific site on GaAs substrate, thus opening the route for the achievement of site controlled GaAs/AlGaAs dots. The method is based on a combination of substrate patterning by LAO and deposition of Ga droplets in a molecular beam epitaxy (MBE) environment.

II. EXPERIMENTAL DETAILS

Our procedure for the deposition of site controlled Ga droplets is based on the idea of fabricating ordered nanoholes on the sample surface by LAO, and then to drive the nucleation of one Ga droplet in each hole, as outlined in Fig. 1: formation of nano-oxide dots on GaAs (001) surface by LAO applying a voltage between the tip of the atomic force microscope (AFM) and the substrate [Fig. 1(b)], subsequent removal of nano-oxide dots and native oxide layer including surface contaminants by wet etching [Fig. 1(c)] and deposition of Ga by MBE with the correct parameters in order to fill each hole with one droplet [Fig. 1(d)]. About this last step, we have to consider that Ga deposited on GaAs at

a)Electronic mail: sergio.bietti@mater.unimib.it

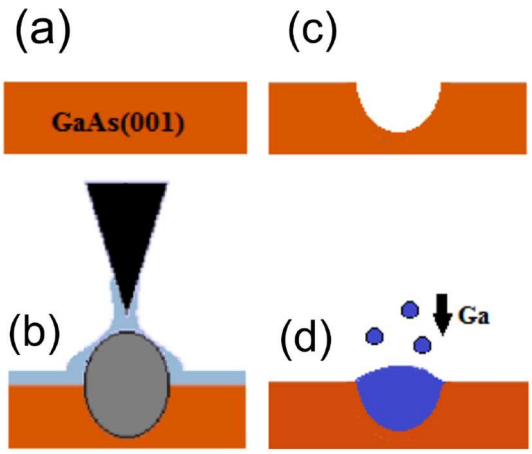

FIG. 1. (Color online) Schematic of the process used for Ga droplet localization: (a) Growth of GaAs(001) buffer layer; (b) LAO process; (c) GaAs after oxide removal; and (d) Ga droplet deposition.

growth temperatures in the range of 200–500 °C spontaneously self-assembles into a spatially disordered ensemble of nanoscale droplets, whose density and size can be tuned through Ga atom flux from effusion cell and substrate temperature.[29,30] Controlling these two parameters, it is possible to tune droplet density in the range between 10^7 and $10^{12}\,cm^{-2}$ (see Ref. 6). Ga desorption is practically insignificant in this temperature range. In order to promote Ga droplet ordering and site control on the GaAs substrate, we performed the growth on a patterned substrate periodically modulated with two dimensional holes.

The fabrication of ordered arrays of nanoholes on the surface was carried out in four steps: (1) a Si-doped GaAs buffer layer with a thickness of 1 μm was grown by MBE on n-doped GaAs (001) substrate to locally produce flat surfaces (0.14 nm RMS). (2) After growth, the GaAs substrate was removed from the MBE chamber and transferred into a programmable AFM system to fabricate the nano-oxide dots using a special conductive tip. This procedure allows to prevent the introduction of surface/interface physical damages.[27] Highly aligned nano-oxide dots were formed on the atomically flat GaAs surface by LAO in tapping mode by applying a bias voltage of 10 V between AFM tip and GaAs surface, with humidity conditions of 60% at room temperature. (3) Oxide nanodot removal by a wet chemical etching (1 min in a solution of HCl (37%):H_2O (1:3), and then rinsing in water). (4) A surface cleaning technique based on wet etching was used to remove any further contaminants on the surface following the procedure outlined in Ref. 31. The deposition of a doped buffer layer on a doped substrate was necessary in order to properly apply voltage pulses between the AFM tip and the sample.

A square lattice pattern with a lattice spacing of 0.8 μm has been realized by LAO. The sample was then introduced into the growth chamber. We performed temperature readings with a thermocouple placed in the rear part of the sample holder and calibrated by observing oxide desorption temperature (at 580 °C) via reflection high energy electron diffraction (RHEED) and by a pyrometer. After oxide removal, 2 nm of GaAs were grown at the same temperature onto the substrate for surface smoothening. Substrate temperature was then decreased to 370 °C and background As pressure decreased below 10^{-9} Torr for the irradiation with Ga flux. Surface reconstruction in flat sample areas, as determined by RHEED pattern, was c(4 × 4). An amount of 1.3 MLs of Ga was then deposited at a rate of 0.02 ML/s. RHEED pattern showed the formation of a Ga-rich (4 × 6) surface reconstruction after the deposition of 1 ML of Ga. Surface morphology for each process step was monitored by AFM measurements, with a tip capable of 7 nm lateral resolution in tapping mode.

III. RESULTS AND DISCUSSION

Figure 2(a) shows the AFM topography of an ordered array of nano-oxide dots fabricated by LAO. The resulting array of nanoholes after oxide wet etching removal is shown in Fig. 2(b) and its Fourier transform in Fig. 2(c). The nanoholes on the patterned substrate are two-dimensionally ordered. In the panel showing Fourier transform image, a large number of narrow satellite peaks in the two dimensional plane are clearly visible, thus explicitly demonstrating the two dimensional long-range ordering of the hole array fabricated by LAO technique.

The depth of the nanoholes depends upon the initial height of the oxide dot (see Fig. 2). This could be explained by the volume expansion effect due to the formation of Ga and As oxides inside the GaAs crystal caused by interdiffusion of OH− during oxidation process.[26,27] We obtained various sizes of oxide dots by varying the oxidation conditions. The dependence of the nanohole depth on the height of oxide dot is linear with a coefficient around 1.2. The nanohole width does not show a noticeable dependence on the oxidation conditions, being almost constant around 400 nm in all our samples. This makes the obtained nanoholes rather shallow, with an aspect ratio (the ratio between height and base of the hole) in the 0.01–0.02 range. The nanoholes show nearly conical shape. The angle α between the axis of revolution and the generatrix of the cone at the bottom of the nanohole, for the typical LAO conditions used in this work, is ≈86° (see Fig. 2).

During the Ga deposition stage on unpatterned substrates, when the Ga flux reaches the c(4 × 4) reconstructed GaAs(001) surface, the first 1 ML of material is incorporated in the substrate to promote the change of the surface to the (4 × 6) Ga stabilized reconstruction. Once the (4 × 6) reconstruction is established on the substrate, droplets start to nucleate at random position.[32] We determined the Ga droplet density behavior on the GaAs(001) flat surface with a series of samples in which Ga droplets were deposited at different substrate temperatures in the range of 200–400 °C, while keeping the Ga flux fixed (0.02 ML/s). The temperature dependence follows an exponential law, as expected by activated diffusion and nucleation processes,[33] with an activation energy of 0.64 ± 0.05 eV (see bottom panel of Fig. 3). The contact angle of the Ga droplets, which gives the intensity of the wetting strength of Ga on the GaAs

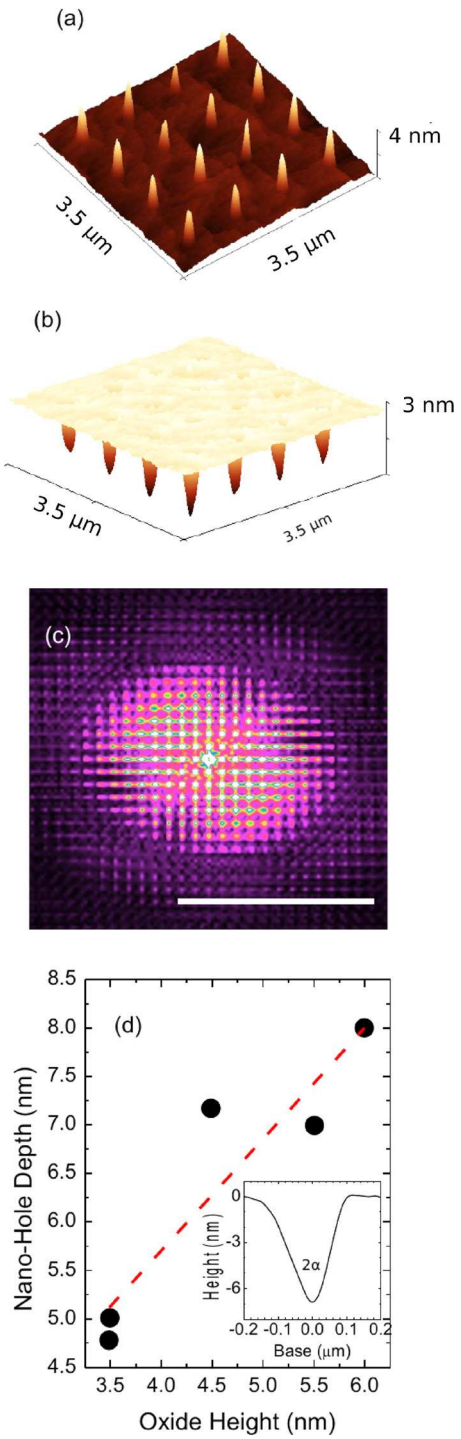

FIG. 2. (Color online) (a) and (b) $3.5 \times 3.5\,\mu m^2$ AFM images of ordered nanoholes obtained after LAO (a) and the corresponding holes arrays after the oxide wet etching (b). (c) Fast Fourier transform of the AFM image shown in (a). The white bar size is $10\,\mu m^{-1}$. (d) Dependence of the nanohole depth after oxide wet etching removal on the oxide dot height after LAO. Inset: Typical nanohole AFM profile.

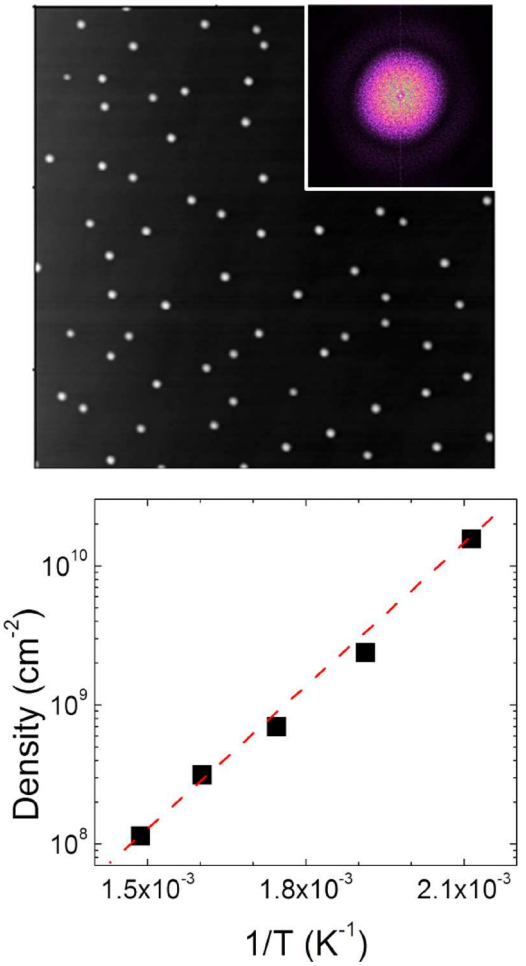

FIG. 3. (Color online) Upper panel: $5 \times 5\,\mu m^2$ AFM image of a Ga droplet grown at T = 370 °C with Ga atom flux of 0.02 ML/s, showing the randomness of the nucleation sites of Ga droplets on flat surface. Inset: Fourier transform of the same AFM image ($50\,\mu m^{-1}$ lateral dimension). Lower panel: Ga droplet density dependence on GaAs substrate temperature.

substrate, measured via *ex-situ* AFM on the flat areas of the sample, is $\beta \approx 45°$.

The AFM image (together with its Fourier transform) of a typical flat GaAs surface after Ga deposition at T = 370 °C is reported in upper panel of Fig. 3. A number of Ga droplets, arranged in a random fashion on the surface, are clearly visible. The absence of correlation is evidenced also in the Fourier transform image. Increasing (decreasing) the substrate temperatures leads to a lower (higher) areal density of larger (smaller) droplets. The droplet spatial arrangement deviates from randomness when substrates, patterned with LAO nanoholes, are used as growth substrates. Figure 4 shows an AFM image of a square array of 4×4 nanoholes with 0.8 μm lattice distance before (panel a) and after (panel b) Ga deposition. In the patterned area, the droplets nucleate within each nanohole with the exception of few droplets which nucleated on the flat areas between the nanoholes. In three cases, two different droplets are nucleated in a single nanohole (see encircled area in Fig. 4). On the flat areas around the pattern, as expected, the Ga droplets randomly nucleate, with an average density determined by the deposition conditions. The observed droplet configuration is statistically significant. As quantitative proof we performed a standard "null hypothesis test."[34] We suppose, as null hypothesis, that there is no correlation between the final droplet position and the pattern grid of the holes. In this case, we can naturally expect that the probability of going inside or outside a hole follows a binomial distribution and depends

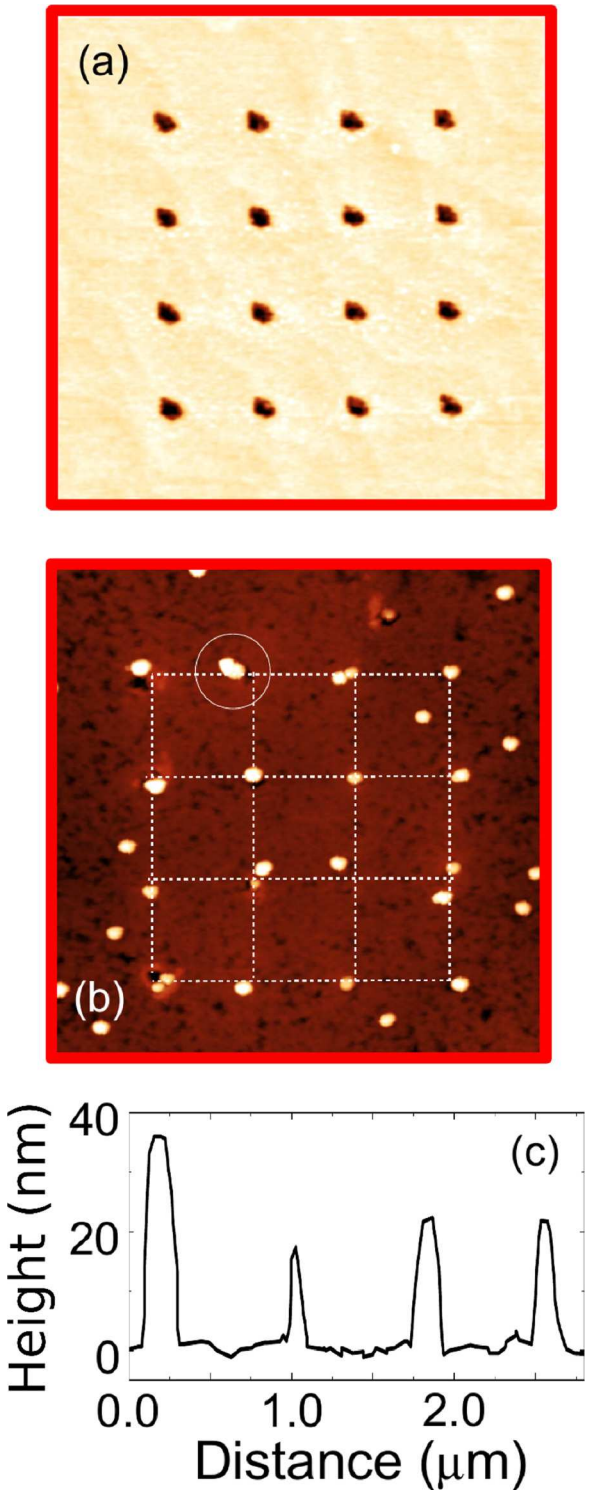

FIG. 4. (Color online) AFM images (4 μm × 4 μm) of the patterned substrate before (a) and after (b) Ga deposition. Here the dashed lines are a guide for the eyes to identify the position of the ordered array of nanoholes templates in the two images. (c) AFM line scan of the same area along the right edge of the nanohole array in (b).

only on the area of the two zones. We consider the area of the AFM image reported in Fig. 4. In that area, the pattern grid consists on $n = 16$ nanoholes with an average radius $R = 200$ nm. Accordingly, the total exposed area of the "nanohole zone" will be $A_h = n\pi R^2 \simeq 2\,\mu\text{m}^2$ that is the 12.5% of the total scanned area (16 μm^2). Taking this into account, we can say that, without correlation, the probability for a droplet to nucleate inside a hole is $p = 25/200$. According to our growth conditions, we expect to nucleate $N = 26$ droplets in the considered area. In agreement with our hypothesis of binomial distribution, we expect an average of $\mu = N \cdot p = 3.25$ filled nanoholes with a standard deviation of $\sigma = \sqrt{\mu(1-p)} = 1.69$. In our experiment, we have seen that 16 droplets have filled a nanohole. The probability of such event in the framework of our null hypothesis is $\mathcal{B}(16; 26, 0.125) = 5 \times 10^{-9}$, that means a very unlikely event. With a level of confidence of 1×10^{-8}, we can reject the null hypothesis and say that the nucleation of one droplet inside each nanohole is a very unlikely event and the presence of nanoholes provides a correlation between the final droplet position and the pattern grid of the holes.

We have then to consider the combined action of capillarity and Ga adatom diffusion to explain the nucleation of Ga droplets in the nanoholes. The phenomenon that drives the nucleation of the Ga droplet within the nanoholes is the capillarity condensation, as explained in detail in Ref. 35. The nucleation of a Ga droplet within a nanoholes is driven by the more efficient decrease, with respect to the planar substrate, of the activation energy for the nucleation of the droplets that takes place in presence of conical cavities (see Ref. 35, chapter 12). The nanohole geometry provides the necessary energy advantage to the Ga adatom system for the nucleation at the bottom of the nanohole, but to obtain the nucleation of one droplet in each nanohole, it is also necessary to consider the nucleation kinetics of Ga droplets in order to prevent the droplet nucleation on the flat areas between the nanoholes (droplet density higher than nanohole density) or the presence of unoccupied sites (droplet density lower than nanohole density). This can be achieved if the average distance between self-assembled Ga droplets on GaAs (001) surface is matching the nanohole spacing. As previously reported, the average distance between Ga droplets can be tuned acting on the substrate temperature during the Ga deposition. The nanohole pitch of 0.8 μm requires a droplet density of $\approx 1.6 \times 10^8\,\text{cm}^{-2}$ and therefore a deposition temperature of 370 °C (as shown in Fig. 3, lower panel).

Concerning the occupation of a single nanohole by two droplets, we again use the null-hypothesis test to demonstrate that the configuration obtained is statistically significant. The probability that the first droplet enter in a hole and the second one is localized in the same nanohole is $p_2 = p^2/16$. We found three double droplets over 16 sites, and the probability of such event in the framework of our null hypothesis is $\mathcal{B}(3; 16, 1 \times 10^{-3}) = 5.2 \times 10^{-7}$ that, again, is a very unlikely event. It is worth noting that extrinsic nucleation sites can be introduced during the LAO and etching processes. Small morphological defects at the rim or inside the nanoholes could locally lower the activation energy for the nucleation.[35] This could justify the nucleation in few sites of two different droplets inside or at the rim of the same nanohole.

It is then possible to compare the occupancy of nanoholes obtained in our experiment with some data present in scientific

literature for InAs QDs fabricated in Stranski–Krastanow growth mode. Atkinson *et al.*,[36] using electron-beam lithography and wet or dry etching, reported a frequency of dot occupancy of nanoholes of about 80%, but also a high frequency of nucleation of multiple dots inside the same nanoholes (about 50%). Kiravittaya *et al.*[37] reported a frequency of unoccupied sites around 1% using optical lithography and wet chemical etching. Using DE technique, Bollani *et al.*[38] reported an occupancy of about 80% for single Ga droplets deposited on Si in Fig. 3 substrate patterned by electron-beam lithography and reactive ion etching.

We then conclude that the observed configuration of the Ga droplets cannot be explained by random positioning, but it is due to a combined action of capillarity condensation inside the nanoholes and of Ga adatom diffusion on the surface, as also reported by Bollani *et al.*[38] for the localization of Ga droplets on a patterned Si substrate. Our data are compatible with the results reported in scientific literature, demonstrating that a combination of LAO and DE techniques allows for the localization of Ga droplets with high frequency of site occupancy and low occurrence of double droplet nucleation in the same nanohole.

IV. CONCLUSIONS

In conclusion, we demonstrate the possibility to fabricate uniform, ordered arrays of site controlled Ga droplets. The growth process strongly relies on interplay of: 1) the substrate patterning, in form of a periodically modulated two dimensional nanoholes array; 2) the conditions selected for the deposition of Ga, in order to prevent the nucleation of droplets in the flat area between the nanoholes or the presence of unoccupied sites. The nanohole array fabrication has been performed via LAO. This method allows for the flexible control of nanoholes ordering and for the avoidance of contaminants and defects, which different lithographic techniques, such as electron beam lithography, usually introduce.

ACKNOWLEDGMENT

The research was supported by the CARIPLO Foundation (prj. SOQQUADRO—No. 2011–0362).

[1]N. N. Ledentsov, Semicond. Sci. Technol. **26**, 014001 (2011).
[2]M. Jo, T. Mano, and K. Sakoda, Cryst. Growth Des. **11**, 4647 (2011).
[3]A. J. Shields, Nat. Photonics **1**, 215 (2007).
[4]N. Koguchi, S. Takahashi, and T. Chikyow, J. Cryst. Growth **111**, 688 (1991).
[5]N. Koguchi and K. Ishige, Jpn. J. Appl. Phys., Part 1 **32**, 2052 (1993).
[6]M. Jo, T. Mano, Y. Sakuma, and K. Sakoda, Appl. Phys. Lett. **100**, 212113 (2012).
[7]C. Somaschini, S. Bietti, N. Koguchi, and S. Sanguinetti, Nano Lett. **9**, 3419 (2009).
[8]S. Adorno, S. Bietti, and S. Sanguinetti, J. Cryst. Growth **378**, 515 (2013).
[9]S. Bietti, C. Somaschini, S. Sanguinetti, N. Koguchi, G. Isella, and D. Chrastina, Appl. Phys. Lett. **95**, 241102 (2009).
[10]L. Cavigli *et al.*, Appl. Phys. Lett. **100**, 231112 (2012).
[11]K. Watanabe, N. Koguchi, and Y. Gotoh, Jpn. J. Appl. Phys. **39**, L79 (2000).
[12]T. Kuroda, S. Sanguinetti, M. Gurioli, K. Watanabe, F. Minami, and N. Koguchi, Phys. Rev. B **66**, 121302(R) (2002).
[13]V. Mantovani, S. Sanguinetti, M. Guzzi, E. Grilli, M. Gurioli, K. Watanabe, and N. Koguchi, J. Appl. Phys. **96**, 4416 (2004).
[14]T. Mano, M. Abbarchi, T. Kuroda, C. A. Mastrandrea, A. Vinattieri, S. Sanguinetti, K. Sakoda, and M. Gurioli, Nanotechnology **20**, 395601 (2009).
[15]M. Jo, T. Mano, M. Abbarchi, T. Kuroda, Y. Sakuma, and K. Sakoda, Cryst. Growth Des. **12**, 1411 (2012).
[16]C. Heyn, A. Stemmann, T. Koppen, C. Strelow, T. Kipp, M. Grave, S. Mendach, and W. Hansen, Appl. Phys. Lett. **94**, 183113 (2009).
[17]C. Heyn, A. Stemmann, T. Koppen, C. Strelow, T. Kipp, M. Grave, S. Mendach, and W. Hansen, Nanoscale Res. Lett. **5**, 576 (2010).
[18]M. Pfeiffer, K. Lindfors, C. Wolpert, P. Atkinson, M. Benyoucef, A. Rastelli, O. G. Schmidt, H. Giessen, and M. Lippitz, Nano Lett. **10**, 4555 (2010).
[19]P. Atkinson, E. Zallo, and O. G. Schmidt, J. Appl. Phys. **112**, 054303 (2012).
[20]K. Hennessy, A. Badolato, M. Winger, D. Gerace, M. Atatüre, S. Gulde, S. Fält, E. L. Hu, and A. Imamolu, Nature **445**, 896 (2007).
[21]H. Lan and Y. Ding, Nano Today **7**, 94 (2012).
[22]H. Heidemeyer, C. Muller, and O. Schmidt, J. Cryst. Growth **261**, 444 (2004).
[23]P. Atkinson, S. Kiravittaya, M. Benyoucef, A. Rastelli, and O. G. Schmidt, Appl. Phys. Lett. **93**, 101908 (2008).
[24]T. Tran, A. Muller, C. K. Shih, P. S. Wong, G. Balakrishnan, N. Nuntawong, J. Tatebayashi, and D. L. Huffaker, Appl. Phys. Lett. **91**, 133104 (2007).
[25]J. Martín-Sánchez *et al.*, ACS Nano **3**, 1513 (2009).
[26]Y. Okada, S. Amano, M. Kawabe, B. N. Shimbo, and J. S. Harris, J. Appl. Phys. **83**, 1844 (1998).
[27]S. W. Koch, M. Kira, G. Khitrova, and H. M. Gibbs, Nat. Mater. **5**, 523 (2006).
[28]J. Martín-Sánchez, P. Alonso-González, J. Herranz, Y. González, and L. Gonzales, Nanotechnology **20**, 125302 (2009).
[29]S. Bietti, C. Somaschini, N. Koguchi, C. Frigeri, and S. Sanguinetti, J. Cryst. Growth **323**, 267 (2011).
[30]C. Somaschini, S. Bietti, N. Koguchi, F. Montalenti, C. Frigeri, and S. Sanguinetti, Appl. Phys. Lett. **97**, 053101 (2010).
[31]J. Tommila, A. Tukiainen, J. Viheriälä, A. Schramm, T. Hakkarainen, A. Aho, P. Stenberg, M. Dumitrescu, and M. Guina, J. Cryst. Growth **323**, 183 (2011).
[32]S. Sanguinetti and N. Koguchi, *Molecular Beam Epitaxy*, edited by M. Henini (Elsevier, Oxford, 2013), pp. 95–111.
[33]J. A. Venables, G. D. T. Spiller, and M. Hanbucken, Rep. Prog. Phys. **47**, 399 (1984).
[34]J. Taylor, *An Introduction to Error Analysis: The Study of Uncertainties in Physical Measurements* (University Science Book, Herndon, 1996).
[35]B. Mutaftschiev, *The Atomistic Nature of Crystal Growth*, Springer Series in Materials Science Vol. 43 (Springer Berlin Heidelberg, Berlin, Heidelberg, 2001).
[36]P. Atkinson, S. P. Bremner, D. Anderson, G. A. C. Jones, and D. A. Ritchie, J. Vac. Sci. Technol., B **24**, 1523 (2006).
[37]S. Kiravittaya, A. Rastelli, and O. G. Schmidt, Appl. Phys. Lett. **87**, 243112 (2005).
[38]M. Bollani *et al.*, Nanotechnology **25**, 205301 (2014).